NAVAL POSTGRADUATE SCHOOL
Monterey, California

UNITED STATES NAVY
· NAVAL POSTGRADUATE SCHOOL ·

THESIS

INVESTIGATIONS OF SELF-PUMPED
PHASE CONJUGATE LASER BEAMS
AND COHERENCE LENGTH

by

George M. Sutton

March, 1993

Thesis Advisor: Oscar Biblarz

Approved for public release: distribution is unlimited.

REPORT DOCUMENTATION PAGE	Form Approved OMB No. 0704-0188

1a. REPORT SECURITY CLASSIFICATION UNCLASSIFIED	1b. RESTRICTIVE MARKINGS

2a. SECURITY CLASSIFICATION AUTHORITY	3. DISTRIBUTION/AVAILABILITY OF REPORT
2b. DECLASSIFICATION/DOWNGRADING SCHEDULE	Approved for public release: distribution is unlimited.

4. PERFORMING ORGANIZATION REPORT NUMBER(S)	5. MONITORING ORGANIZATION REPORT NUMBER(S)

6a. NAME OF PERFORMING ORGANIZATION Naval Postgraduate School	6b. OFFICE SYMBOL (If applicable) 31	7a. NAME OF MONITORING ORGANIZATION Naval Postgraduate School

6c. ADDRESS (City, State, and ZIP Code) Monterey, California 93943-5000	7b. ADDRESS (City, State, and ZIP Code) Monterey, California 93943-5000

8a. NAME OF FUNDING/SPONSORING ORGANIZATION	8b. OFFICE SYMBOL (If applicable)	9. PROCUREMENT INSTRUMENT IDENTIFICATION NUMBER

8c. ADDRESS (City, State, and ZIP Code)	10. SOURCE OF FUNDING NUMBERS			
	PROGRAM ELEMENT NO.	PROJECT NO.	TASK NO.	WORK UNIT ACCESSION NO.

11. TITLE (Include Security Classification)
INVESTIGATIONS OF SELF-PUMPED PHASE CONJUGATE LASER BEAMS AND COHERENCE LENGTH (Unclassified)

12. PERSONAL AUTHOR(S)
Sutton, George M.

13a. TYPE OF REPORT Master's Thesis	13b. TIME COVERED FROM ____ TO ____	14. DATE OF REPORT (Yr., Mo., Day) March, 1993	15. PAGE COUNT 54

16. SUPPLEMENTARY NOTATION: The views expressed in this thesis are those of the author and do not reflect the official policy or position of the Department of Defense or the U.S. Government.

17. COSATI CODES			18. SUBJECT TERMS (Continue on reverse if necessary and identify by block number)
FIELD	GROUP	SUB-GROUP	Coherence Length, Photorefractive Effect, Barium Titanate, Self-Pumped Phase Conjugation

19. ABSTRACT (Continue on reverse if necessary and identify by block number)
The phase conjugation process by a nonlinear, photorefractive crystal is not completely ideal and losses should be expected to occur after a beam is conjugated. This thesis research investigates possible changes in coherence length as a result of internal losses in barium titanate ($BaTiO_3$). Additionally, laser reflections from a corner cube reflector is also examined for changes in coherence length. Experimental findings are inconclusive because the conventional spectrometer used to measure coherence length did not possess the required resolution. It is recommended that an interferometer which can resolve the laser line width be utilized for future coherence length measurements, together with a means of blocking the conjugated beam from entering the laser cavity and destabilizing the oscillations within.

20. DISTRIBUTION/AVAILABILITY OF ABSTRACT ■ UNCLASSIFIED/UNLIMITED □ SAME AS RPT. □ DTIC USERS	21. ABSTRACT SECURITY CLASSIFICATION Unclassified

22a. NAME OF RESPONSIBLE INDIVIDUAL Oscar Biblarz	22b. TELEPHONE (Include Area Code) 408-656-3096	22c. OFFICE SYMBOL AA/Bi

DD Form 1473, JUN 86   Previous editions are obsolete.   SECURITY CLASSIFICATION OF THIS PAGE
S/N 0102-LF-014-6603

i

UNCLASSIFIED

INVESTIGATIONS OF SELF-PUMPED PHASE
CONJUGATE LASER BEAMS AND COHERENCE LENGTH

by

George M. Sutton
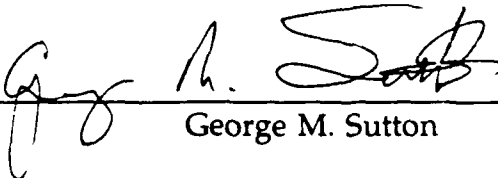Lieutenant, United States Navy
B.S., Southern University, 1986

Submitted in partial fulfillment of the
requirements for the degree of
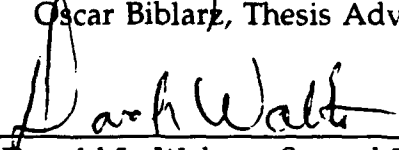
MASTER OF SCIENCE IN PHYSICS
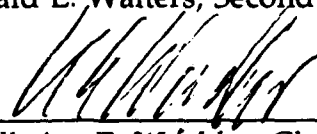
from the

NAVAL POSTGRADUATE SCHOOL
March, 1993

Author: _____
George M. Sutton

Approved by: _____
Oscar Biblarz, Thesis Advisor

_____
Donald L. Walters, Second Reader

_____
Karlheinz E. Woehler, Chairman
Department of Physics

ABSTRACT

The phase conjugation process by a nonlinear, photorefractive crystal is not completely ideal and losses should be expected to occur after a beam is conjugated. This thesis research investigates possible changes in coherence length as a result of internal losses in barium titanate ($BaTiO_3$). Additionally, laser reflections from a corner cube reflector is also examined for changes in coherence length. Experimental findings are inconclusive because the conventional spectrometer used to measure coherence length did not possess the required resolution. It is recommended that an interferometer which can resolve the laser line width be utilized for future coherence length measurements, together with a means of blocking the conjugated beam from entering the laser cavity and destabilizing the oscillations within.

Accesion For		
NTIS CRA&I		☒
DTIC TAB		☐
Unannounced		☐
Justification		
By		
Distribution /		
Availability Codes		
Dist	Avail and / or Special	
A-1		

iii

ACKNOWLEDGEMENTS

I would like to thank Professor Biblarz for his support and guidance throughout my research. I am also appreciative to Dr. Hossin Abeledeyem of Marshall Space Flight Center for his assistance in performing the phase conjugation experiments for this thesis. Finally, I am especially grateful to my wife, DeAnne, for her unfailing support during my tenure here at the Naval Postgraduate School.

TABLE OF CONTENTS

vi

I. INTRODUCTION

Optical phase conjugation (OPC) is a process that involves the use of a large variety of nonlinear optical phenomena to reverse the direction of propagation of a light beam. Phase conjugate waves can be produced by the following nonlinear interactions: photorefraction, stimulated Brillouin scattering, stimulated Raman scattering, and photon scattering. The major thrust of optical phase conjugation is in the area of adaptive optics but potential applications also exist in image processing, fiber-optic communications, laser resonators, target tracking and image amplification.

Photorefractive crystals such as barium titanate ($BaTiO_3$), lithium niobate ($LiNbO_3$), and potassium niobate ($KNbO_3$) to obtain phase conjugate reflections have all proven to be the most effective conjugators at low intensity levels. These crystals posses large nonlinear coefficients which enables the experiments to exploit the principle of the photorefractive effect; a topic that will be discussed later in section IIC. These crystals are also capable of acting as optical film for applications in real time holography.

The demonstration of phase conjugation in the photorefractive crystal $BaTiO_3$ has been accomplished by numerous methods such as: externally pumped four-wave mixing, self-pumped phase conjugation, and mutually pumped phase conjugation. Self-pumped phase conjugation is the only of the above methods

1

which utilizes a single incident beam to generate a phase conjugate beam. Applications of phase conjugation in optical communications and strategic laser weapons require only one incident laser beam and no external pumping beams. $BaTiO_3$ is unique because self generated conjugate returns are relatively easy to obtain.

Although most experimental investigations have addressed the phase conjugate process within the crystal, very little attention has been given to the quality of the phase conjugated beam. According to [Ref. 1], the process of phase conjugation is not expected to produce total reversibility, so a "penalty" in the decrease of coherence length is sought. This thesis evaluates the temporal fidelity of the phase conjugation process using $BaTiO_3$ and attempts to measure coherence length changes of phase conjugated laser beams. Results obtained in these experiments could apply to high power lasers operating in space as well as to low power lasers operating in fiber optic communications.

The phase conjugation experiments performed for this study were conducted at Marshall Space Flight Center (MSFC) as a part of the Naval Postgraduate School's experience tour program. The optical laboratory facilities and $BaTiO_3$ crystal utilized at MSFC were paramount in the attempt at answering the coherence length measurements for this study.

II. THEORY AND BACKGROUND

A. PHASE CONJUGATION

Optical phase conjugation (OPC) is the process of creating a complex conjugate of an electromagnetic wave. Fisher [Ref. 2] defines OPC as "A technique that incorporates nonlinear optical effects to precisely reverse both the direction of propagation and the overall phase factor for each plane wave in an arbitrary beam of light." This process can be regarded as a special kind of smart mirror with an unusual reflection and image transformation properties. A phase conjugate mirror (PCM) in comparison to an ordinary mirror is depicted in Figure 1.1. This figure illustrates the difference between reflection directions of a diverging beam. Ordinary reflection conjugates normal component and OPC mirror conjugates both normal and tangential components.

The mathematical significance of phase conjugation can be seen by considering an optical wave propagating through a linear lossless, distorting medium in the +z direction. The electric field $E_1(r,t)$ is:

$$E_1(r,t) = RE[\psi(r)e^{i(\omega t - \kappa z)}] \tag{1-1}$$

3
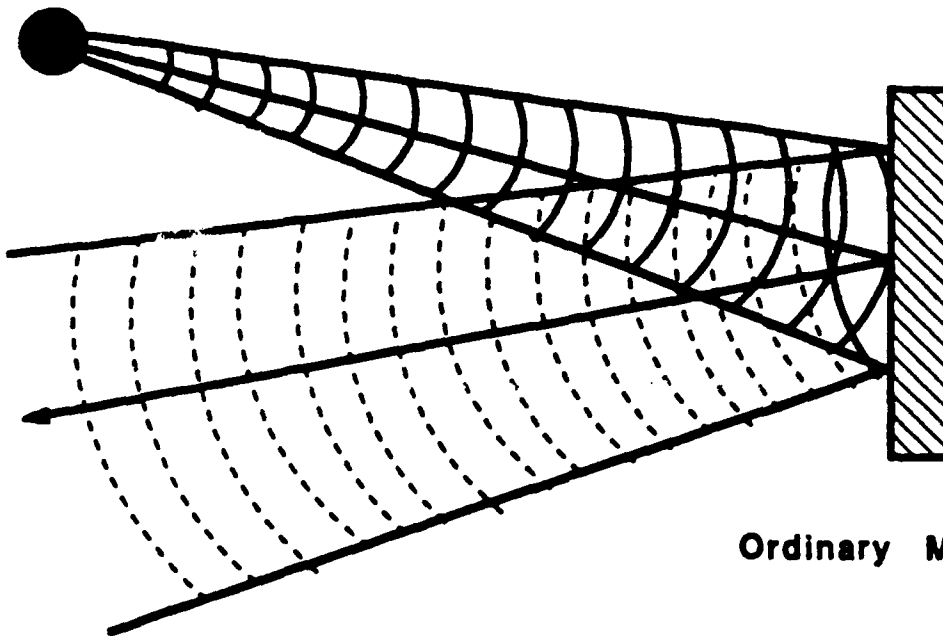
Figure 1.1. Comparison of a spherical wave reflection from an ordinary mirror and a phase conjugate mirror. [Ref. 3]
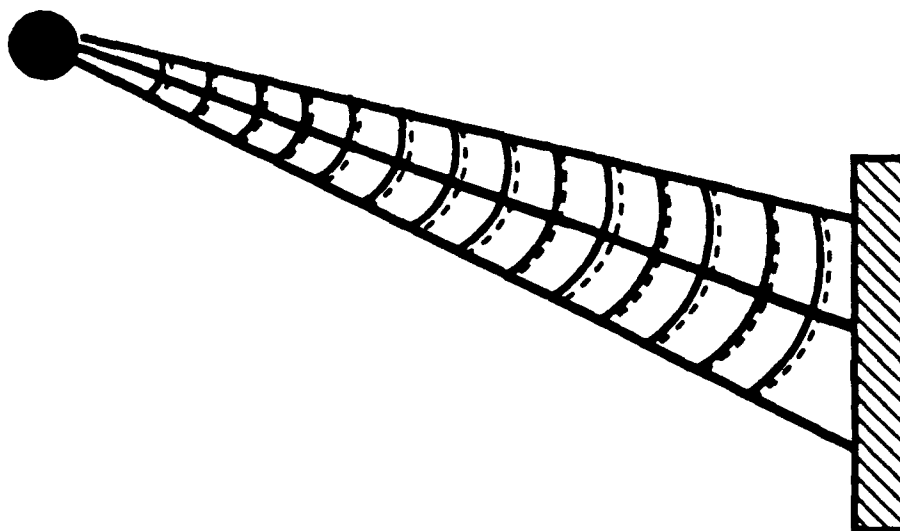
4

The dependence of Ψ on r reflects the spatial information it carries and the effects of distortion. If an optical field $E_2(r,t)$ is generated in such a way that the real part of $E_2(r,t)$ is the complex conjugate of the spatial part of $E_1(r,t)$ then the wave is called the phase conjugate of $E_1(r,t)$, i.e.,

$$E_2(r,t) = RE[\psi^*(r)e^{i(\omega t + \kappa z)}] \qquad (1\text{-}2)$$

Since the wavefronts of $E_2(r,t)$ coincide everywhere with those of $E_1(r,t)$ but propagate in the reverse direction, it looks like a movie running backwards; hence the phase conjugate of E_1 is also called the 'time reversal' of E_1. [Ref. 3]

B.   WAVE EQUATION IN NONLINEAR MEDIUM

The propagation of an optical wave through a medium is described by Maxwell's equations, [Ref. 4]

$$\nabla \times E = -\frac{\partial B}{\partial t} \qquad (1\text{-}3)$$

$$\nabla \times H = J + \frac{\partial D}{\partial t}, \qquad (1\text{-}4)$$

where E, D, B, and H are the usual electric and magnetic vectors associated with the electromagnetic wave and J is the current density. The electric and magnetic field vectors can also be written as,

5

$$D = \varepsilon_o E + P \qquad (1\text{-}5)$$

$$B = \mu_o H + M , \qquad (1\text{-}6)$$

where ε_o and μ_o are respectively the permittivity and permeability of free space. M is the magnetization vector and the total polarization vector P is a combination of its linear and nonlinear components. P can be written as

$$P = P_L + P_{NL} , \qquad (1\text{-}7)$$

where the linear part of the polarization is:

$$P_L = \varepsilon_c \chi^{(1)} E , \qquad (1\text{-}8)$$

and the nonlinear polarization is:

$$P_{NL} = \chi^{(2)} E^2 + \chi^{(3)} E^3 + ... \qquad (1\text{-}9)$$

The linear susceptibility $\chi^{(1)}$ produces gain, absorption, index of refraction, and birefringence. The second-order susceptibility leads to second harmonic generation, the Pockell's effect, and parametric mixing. The third-order susceptibility term allows third harmonic generation, stimulated Brillouin scattering, three wave mixing, four wave mixing, and Kerr effects. [Ref. 5]

Equation 1-4 can be rewritten as:

$$\nabla \times H = \sigma E + \frac{\varepsilon \partial}{\partial t} E + \frac{\partial}{\partial t} P_{NL} , \qquad (1\text{-}10)$$

where σ is the conductivity, and ($\varepsilon = \varepsilon_o(1 + \chi^{(1)})$) is the linear dielectric permittivity. By using differential manipulations and assuming $M=0$ and $\sigma=0$, equation 1-10 reduces to:

$$\nabla^2 E - \mu_o \varepsilon \frac{\partial^2 E}{\partial t^2} = \mu_o \frac{\partial^2 P_{NL}}{\partial t^2} \; . \tag{1-11}$$

Equation 1-11 shows how an electric field can evolve in the presence of a nonlinear polarization. In the absence of such a polarization, the right side of the equation is zero and Equation 1-11 reduces to the standard wave equation. [Ref. 4]

$$\nabla^2 E - \mu_o \varepsilon \frac{\partial^2 E}{\partial t^2} = 0. \tag{1-12}$$

Using the expression for the electric field in Equation 1-1, Equation 1-12 can be written as:

$$\nabla^2 \psi + [\omega^2 \mu_o \varepsilon - \kappa^2]\psi - 2ik\psi = 0 \; , \tag{1-13}$$

and the complex conjugate is,

$$\nabla^2 \psi^* + [\omega^2 \mu_o \varepsilon^* - \kappa^2]\psi^* + 2ik\psi^* = 0 \; . \tag{1-14}$$

The above equation is the wave equation that decribes the propagation of the phase conjugate electric field in Equation 1-2. Equation 1-14 describes the propagation of a field having the same equiphase surfaces at each point in space

and propagating in a direction opposite to that of the incident wave in Equation 1-1.

An application of a phase conjugate mirror to restore aberrated wavefronts to their initial shape is shown if Figure 1.2. In Figure 1.2, an incident beam, after propagating through a distoring medium, yields an aberrated phase front. After the interaction with the PCM and subsequent passage back through the same distorting medium, the initial planar wavefront is recovered. The above concept is known as the distortion correction property of phase conjugation.

C. THE PHOTOREFRACTIVE EFFECT

The photorefractive effect induces changes in the refractive index of electro-optic materials. [Ref. 6] It is based on the photoexcitation of free carriers, which then diffuse or drift in an externally applied electric field away from the light beam to trapping sites. The resulting redistribution of charges gives rise to space charge fields within the nonlinear medium in the illuminated areas. The generated space-charge field E results in a change of refractive index, via the linear electro-optic effect. This change in the index of refraction is semi-permanent such that it may last from milliseconds to months, depending of the nonlinear material. The photorefractive effect is material dependent and may be induced by ultraviolet, visible or infrared radiation. [Ref. 6]

The mechanism that gives rise to the photorefractive effect is basically a three step process and described by Pepper. [Ref. 3] The effect occurs in materials
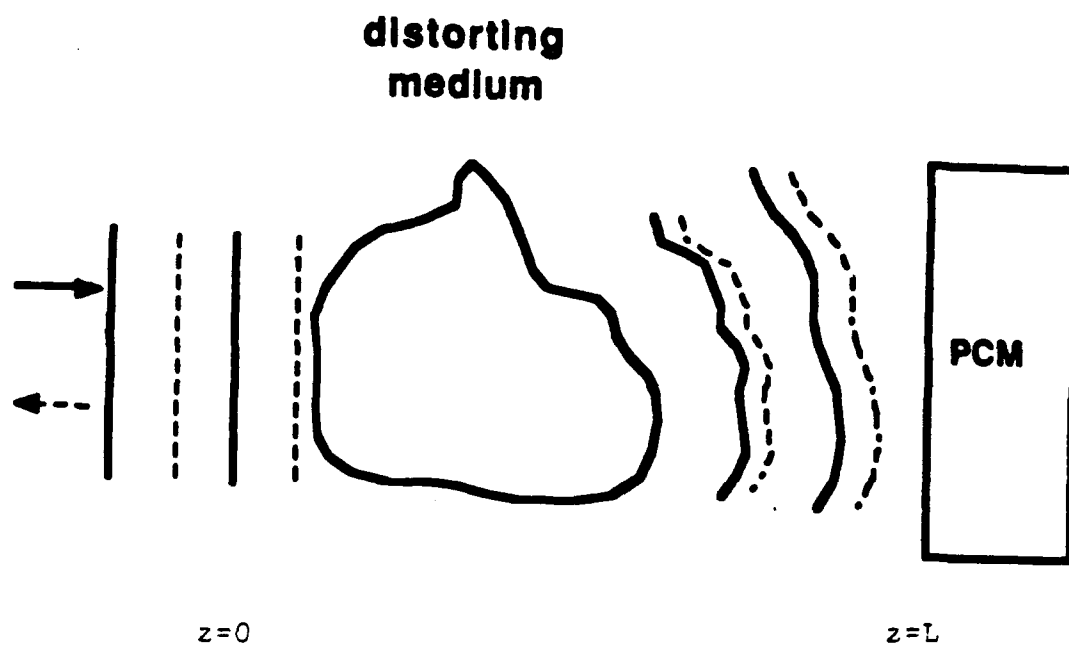
Figure 1.2. Illustration of distortion correction by a phase conjugate mirror. [Ref. 3]

that have localized charge states (traps) in the energy gap between the valence and conduction bands.

1. Incident photons excite charges into the conduction bands where they can drift and/or diffuse into another trap. Since the retrapping occurs at random and the excitation is most probable at an intensity maximum, there is a net migration or a separation of charge.

2. This spatially dependent separation of charge gives rise to strong electrostatic fields.

3. This electrostatic field then creates a spatially varying refractive index change via the linear electrooptic effect and thus forms a refractive grating. The refractive grating serves as a reflecting surface for incoming light that produces a phase conjugated light beam.

In order to quantitatively explain the concepts of the photorefractive phenomena, a simple model is utilized. In this model the photorefractive medium is assumed to contain certain types of impurities or imperfections. Such ionized impurities are capable of capturing electrons. It is also assumed that the density of donor impurity be N_D and $N_D{}^i$ is the density of ionized donor impurity. The rate of electron generation is $(sI+\beta)(N_o-N_o^i)$ and the rate of trap capture is $\gamma_R N N_D{}^i$ where,

N — electron density;

s — cross section for photoexcitation;

I — light intensity;

β — rate of thermal generation of electrons;

γ_R — electron-ionized trap recombination rate.

The rate equation for $N_D{}^i$ can be written as

10

$$\frac{\partial N^{i_D}}{\partial t} = sI(N_D - N_D^i) - \gamma_R N N_D^i \ . \tag{1-15}$$

The rate of generation of electrons is the same as that of the ionized impurities except that the electrons are mobile and the impurities are stationary. The rate equation for electron density can be written as: [Ref. 8]

$$\frac{\partial N}{\partial t} - \frac{\partial N_D^i}{\partial t} = \frac{1}{q}\nabla \cdot j \ , \tag{1-16}$$

The current density j consists of contributions from the drift of charge carriers and diffusion, which is due to the gradient of carrier density. The equation for current density can be written as:

$$j = qN\mu E + k_B T\mu \nabla N \ , \tag{1-17}$$

where,

μ — mobility factor;

E — electric field;

$k_B T$ — product of Boltzman's constant and Temp.

The electric field will obey the following Maxwell's equation:

$$\nabla \varepsilon E = \rho^{(r)} = -q(N + N_A - N_D^i) \ , \tag{1-18}$$

where ε is the permittivity, $\rho^{(r)}$ the charge density and N_A is the density of acceptor impurity.

In the absence of light illumination the charge neutrality can be written as:

If N is small, then $N_D^i = N_A$ in the absence of light. [Ref. 7]

11

$$(N + N_A - N_D^i) = 0 .$$
(1-19)

On the other hand, if the photorefractive medium is illuminated, bright regions will be formed by the absorption of photons Dark regions will be formed by the trapping of the remainder of positively charged ionized donor impurities. This process leads to a charge separation which induces a space-charge electric field. The space-charge electric field causes a change in the index of refraction and subsequently forms a grating.

For the photorefractive effect to exist, the generation of a large number of charged carriers is required (typically 10^{15} per cm^3). The speed of refractive index changes and subsequent grating formation is limited by the finite time required to absorb a large number of photons.

D. WAVE MIXING IN PHOTOREFRACTIVE MEDIA

If two beams of coherent electromagnetic radiation (lasers) are incident upon a photorefractive crystal and intersect inside the crystal, a variation of intensity due to the photorefractive effect will induce a volume index grating. This volume index grating wave vector can be written as

$$\kappa = \pm(\kappa_2 - \kappa_1) ,$$
(1-20)

where κ_1, κ_2 are wave vectors of the beams. With the presence of these gratings, the propagation of the coherent beams leads to strong diffraction inside the medium. In other words, when beam 1 is scattered by the index grating, the

12

diffracted beam propagates along the direction of beam 2. Similarly, when beam 2 is scattered by the same index grating, the diffracted beam propagates along beam 1. This 'wave mixing' phenomenon in photorefractive media can occur by two processes: two-wave mixing and four-wave mixing.

1. Two-Wave Mixing

Two-Wave mixing or two-beam coupling is the basic interaction of two propagating waves inside a photorefractive medium. A schematic of two-wave mixing can be seen in Figure 1.3. In order to explain two-wave mixing mathematically, consider two coherent beams inside a photorefractive medium whose electric field vectors can be expressed by:

$$E_1 = A_1 e^{i(\omega t - \kappa_1 \tau)} \tag{1-21}$$

$$E_2 = A_2 e^{i(\omega t - \kappa_2 \tau)} , \tag{1-22}$$

where A_1 and A_2 are the wave amplitudes, ω the angular frequency, and κ_1 and κ_2 are the wave vectors. At the intersection of these two beams inside the medium, a volume index grating is formed as discussed earlier. The changing index of refraction can be written as,

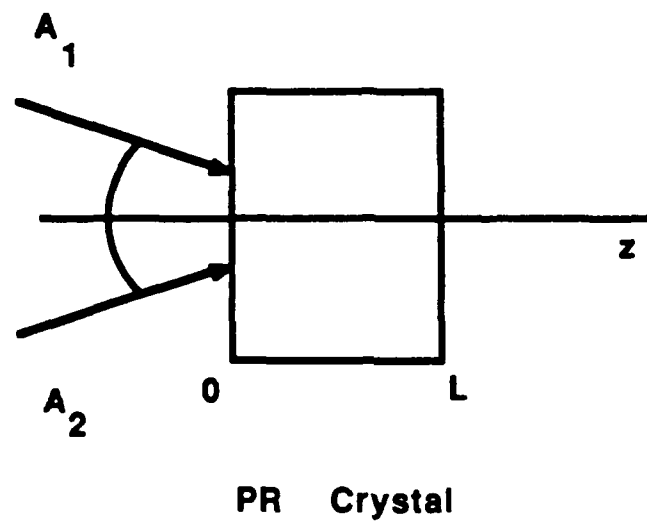$$n = n_o + \frac{\phi_o}{I_o} e^{(-i\kappa\tau)} , \tag{1-23}$$

13

Figure 1.3. Schematic diagram of two-wave mixing in a photoreactive material.
[Ref. 3]

14

where $I_o=I_1+I_2=|A_1|^2+|A_2|^2$, n_o is the index of refraction when no light is present, and ϕ_o is an amplitude phase parameter. [Ref. 7] This phase parameter indicates the degree to which the index grating is shifted spatially with respect to the light interference pattern. The presence of the spatial phase shift allows for energy transfer between the two beams. Energy transfer is not always equal between the two beams. Beam 2 can gain more energy from beam 1 with the proper grating spacing and orientation to the crystal axis and vice versa. If the above conditions are satisfied, two-wave mixing can be achieved with amplification of either beam.

2. Four Wave Mixing

Four wave mixing in a photorefractive medium is one of the most popular methods being utilized to obtain phase conjugate waves. In this process, a photorefractive crystal is pumped by a pair of counterpropagating beams. If a signal beam directed into the crystal while the "pumping" process is occurring, a fourth beam will be generated. This fourth beam propagates in an opposite direction than the signal beam does and is time reversed. The basic geometry of phase conjugation is illustrated in Figure 1.4.

15

ψ_1 (nondepleted pump wave)

$\psi_3(o)$

$\psi_3(l)$

Nonlinear medium

$\psi_4(o)$

$\psi_4(l)$

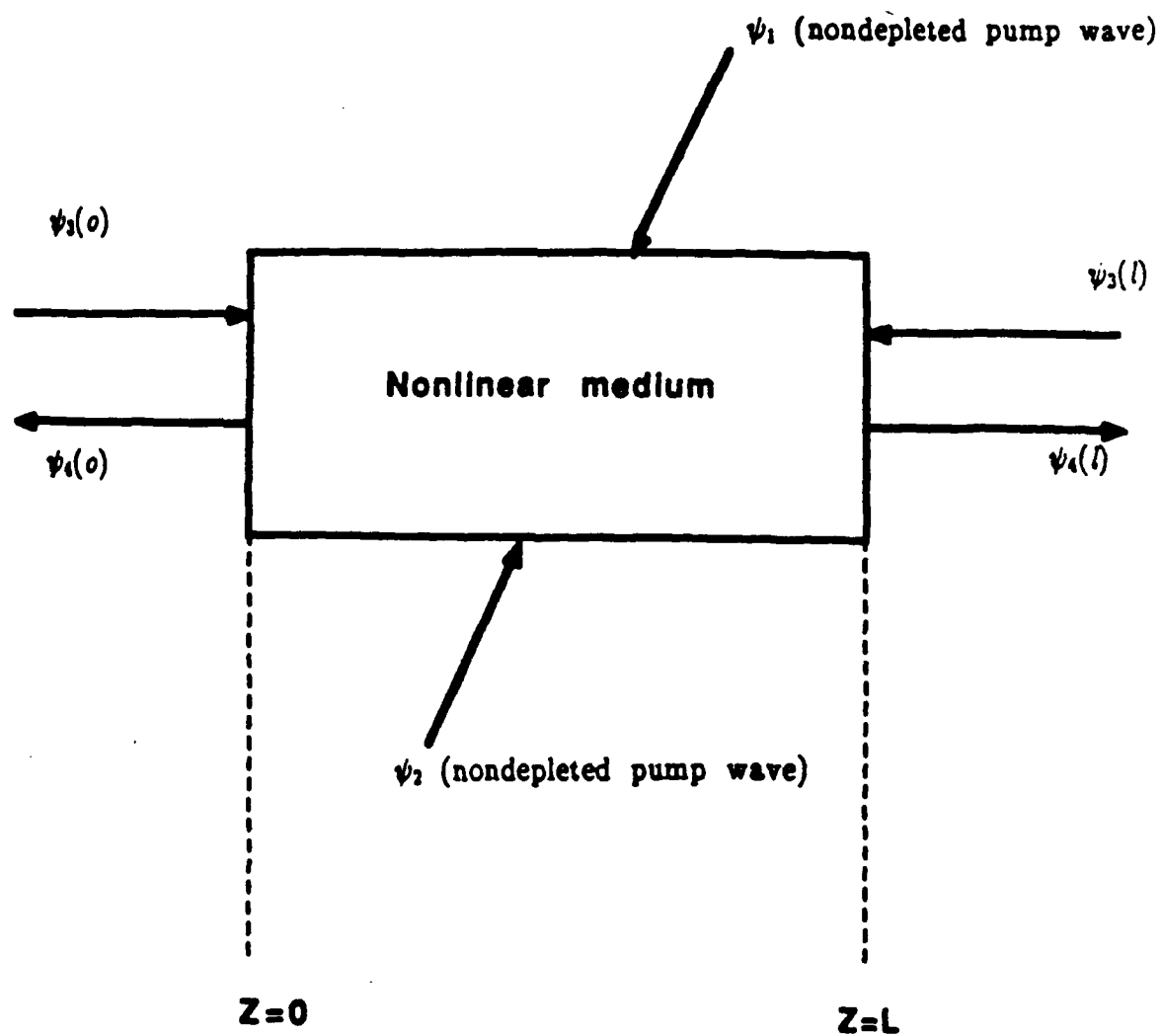ψ_2 (nondepleted pump wave)

Z=0

Z=L

Figure 1.4. Four-Wave Mixing. The basic geometry of optical phase conjugation by four-wave mixing. [Ref. 3]

16

The electric field of the four waves of the same frequency ω as depicted in Figure 1.4 can represented by the following equations:

$$E = \sum_{j=1}^{4} \psi_j e^{i(\omega t - \kappa_j \cdot r)} , \qquad (1\text{-}24)$$

where ψ_1, ψ_2, ψ_3, ψ_4 are the complex amplitudes of the waves, and κ_1, κ_2, κ_3, κ_4 are the wave vectors. ψ_1 and ψ_3 produce a grating that diffracts ψ_2 and generates ψ_4. ψ_4 is the phase conjugate of ψ_3. At the same time ψ_2 and ψ_3 produce a grating that diffracts ψ_1, also generating a contribution to ψ_4. Thus, the phase conjugate beam ψ_4 is the sum of two different contributions of diffraction effects. This is the reason why reflectivities have exceeded unity in many four wave mixing experiments [Ref. 4].

E.   SELF PUMPED PHASE CONJUGATION

When four wave mixing generates a phase conjugate replica of a signal beam, the quality of the phase conjugate beam depends on the alignment of the external pumping beams. Consequently, any misalignment in the pumping beam degrades the fidelity of the phase conjugate beam. This stringent alignment criterion can be reduced by utilizing a 'self-pumping' phase conjugator. In this arrangement the pump beams are generated from the incident beam itself.

Self pumped phase conjugation was first realized by Feinberg [Ref. 8] with the infamous 'CAT' mirror. The pump beams in the Feinberg mirror are derived from the fanning beam fed back by total internal reflections as depicted in Figure

17

1.5. In the interaction there are four beams that allow the phenomena to occur: the input beam, its phase conjugate, and the two beams that act as pump beams. The pumping beam from one interaction region is reflected into the other interaction region by a corner cube or retroreflection. In Figure 1.5, the pumping beams A and A' are generated from the incident beam D. These two beams are internally reflected from adjacent crystal faces near an edge which generates two linking beams B and B'. The two linking beams serve as bridges between the two encircled interaction regions.

Each interaction region contributes to the phase conjugate output wave C. Because the self-generated pump waves have the natural freedom to select angular orientation and spatial distribution that optimizes interaction, this device can exhibit reflectivities of 25% or greater.

In order for a beam to self pump its own phase conjugate beam, the equation below must be satisfied:

$$\alpha L > 2.34,$$

where L is the crystal's interaction length and α is a coupling parameter which depends on the geometry of the optical beams' orientation relative to the crystal axis. The coupling parameter is also dependent on the charge density of the crystal but is independent of the incident beam's intensity. The coupling parameter can be expressed as [Ref. 8]:
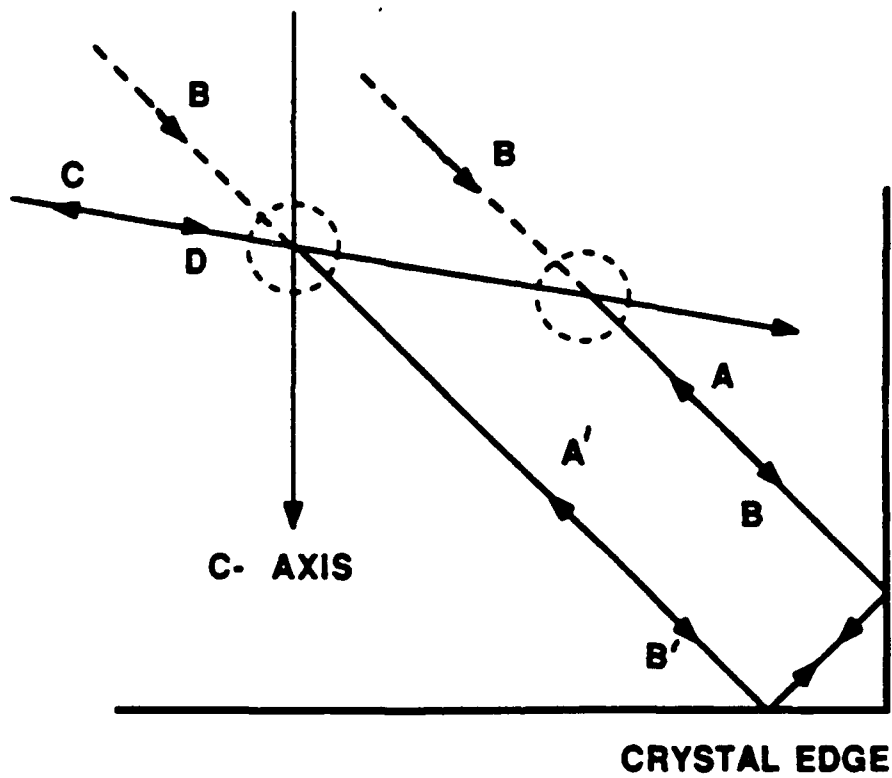
Figure 1.5. Self-pumped optical phase conjugator demonstrated by Fienberg. [Ref. 8]

19

$$\alpha = \left(\frac{w}{2nc}\right)\left[E\, r_{\text{eff}}/\cos(\alpha_1 - \alpha_2)/2\right], \qquad (1\text{-}25)$$

where,

α_1, α_2 — Angle of rays with c axis;

w — optical frequency;

n — index of refraction;

E — electric field;

r_{eff} — Pockels coefficient.

If there is no applied electric field, E is given by:

$$E = (k_B T/q)\left[\frac{K}{1 + \left(\dfrac{K}{K_o}\right)^2}\right], \qquad (1\text{-}26)$$

where q is the charge of the carrier, $k_B T$ the thermal energy and

$$K = 2\left(\frac{nw}{c}\right)\sin\left(\alpha_1 - \frac{\alpha_2}{2}\right)$$

$$K_o = (Nq^2/\varepsilon\varepsilon_o K_B T)^{\frac{1}{2}},$$

In this geometry, N is the number density of charges available for migration, and $\varepsilon\varepsilon_o$ is the static dielectric constant in the direction of the wave vector κ [Ref. 8].

F.   THE BARIUM TITANATE CRYSTAL

Barium titanate is classified as an oxygen-octahedra ferroelectric photoconductive crystal [Ref. 9]. It was one of the first ferroelectric materials to be recognized as photorefractive. The particular advantage of $BaTiO_3$ for photorefractive applications the large value of the electro-optic tensor component r_{42}. This tensor component is responsible for the efficiency of the refractive index grating and also phase conjugate reflectivity.

$BaTiO_3$ has a tetragonal structure at room temperature and undergoes a phase transition to cubic at 130°C. Figure 1.6 illustrates the schematic diagram of the unit cell of $BaTiO_3$ in the cubic phase. The crystal is comprised of Ba^{2+} ions at the cube corners, Ti^{4+} ion at the center, and O^{2-} ions at the face centers. The cubic phase is stable to a temperature of about 9°C at which a transition to an orthorhombic phase occurs. [Ref. 9]

The energy band structure of $BaTiO_3$ is determined by the titanium 3d and oxygen 2p orbitals. The titanium 3d orbitals are responsible for low lying levels of the conduction band and the oxygen 2p orbitals are responsible for the upper levels of the valence band.

1.   Domains and Poling of $BaTiO_3$

Figure 1.7 shows schematically the domain structure of $BaTiO_3$ in the tetragonal phase. Two types of domains are present in the crystal. They are the antiparallel polarization domains and the domains whose polarization lie perpendicular to each other. Both types of domains should be removed prior to
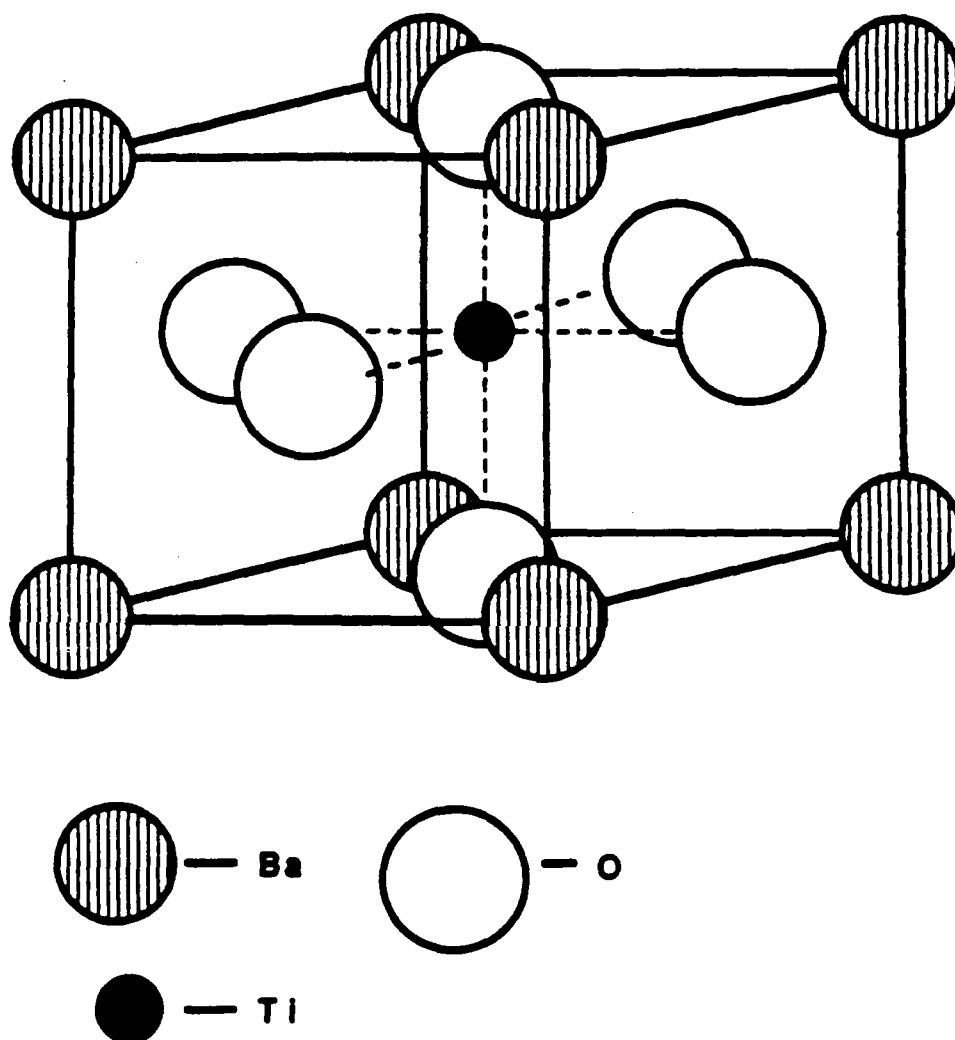
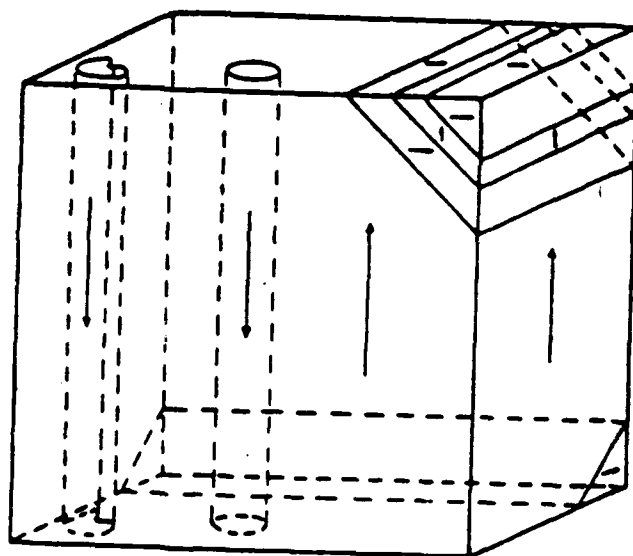**Figure 1.6.** Cubic unit cell structure of BaTiO$_3$ crystal. [Ref. 9]

Figure 1.7. Domain structure of Barium Titanate in tetragonal phase. The arrows represent the direction of polarization. [Ref. 9]

23

illumination to reduce scattering and to achieve a single domain crystal is achieved.

The single domain is achieved by completing the nucleation and movement of the domain walls. To produce a useful electro-optic crystal, two reliable methods to remove domain walls exist.

In the first technique, the perpendicular domains are removed at room temperature by applying mechanical uniaxial pressure alternatively along two different directions. After this mechanical pressure is applied, an electric field is applied along the third direction and the crystal is heated to a temperature below 130°C. [Ref. 9] The electric field is removed from the crystal and is then cooled to room temperature. The removal of the electric field results in the elimination of the parallel domains which in turn produces a single domain crystal.

In the second method, the application of mechanical stress is omitted. The first is to heat the crystal to a temperature above 130°C. Then the crystal is cooled through the cubic tetragonal phase with the presence of an applied electric field. This technique is not widely used because all of the parallel domains aren't removed.

2.   Electro-optic Properties of $BaTiO_3$

The index of refraction for barium titanate is 2.44 for ordinary rays and 2.365 for extraordinary rays at 514.5 nm. [Ref. 10] The dielectric constants at room temperature are 135 parallel to the c-axis and 3700 perpendicular to the c axis

[Ref. 11]. The non-zero elements of the electro-optic tensor are 80 pm/V for r_{33}, 24 pm/V for r_{13}, and 1640 pm/V for r_{42}. [Ref. 5]

G.   LASER COHERENCE

Laser coherence length is the distance at which light waves remain in phase as they travel through space. All forms of light have some degree of temporal coherence, but only over a characteristic 'coherence length'. This coherence length is very close to zero for incandescent light bulbs and can be many meters for lasers. The coherence length depends on the nominal wavelength (λ) and on the wavelength's width of distribution ($\Delta\lambda$) or: [Ref. 11]

$$Coherence\ length = \frac{\lambda^2}{2\Delta\lambda}$$

The above equation can be written as a function of linewidth ($\Delta\lambda$) by using the following relationship:

$$\Delta\upsilon = \frac{c}{\lambda^2}\Delta\lambda$$

Then,

$$Coherence\ Length = \frac{c}{2\Delta\upsilon}.$$

25

III. EXPERIMENTAL INVESTIGATION

A. OVERVIEW

The objective of this experiment was an attempt to measure the temporal-coherence properties of an incident laser beam and then to try to evaluate the temporal fidelity of the self-pumped phase conjugation process using barium titanate. Additionally, a comparison was also made measuring temporal properties of a laser that was specularly reflected from a corner-cube reflector. Based on these measurements a determination was made on the effectiveness of measuring the temporal-coherence properties of a self-pumped phase conjugate laser beam using conventional laser spectrometers.

B. PHASE CONJUGATE COHERENCE LENGTH MEASUREMENTS

The first experiment was conducted at Alabama A&M University's Optics Lab with personnel from Marshall Space Flight Center (MSFC). The $BaTiO_3$ crystal used for this experiment was obtained from Sanders and Associates. The crystal measured 0.5 x 0.5 x 0.5 cm. It had been mechanically stressed at the factory and electrically poled by technicians at the MSFC laboratory. The crystal axis was oriented 45° to the incident laser radiation.

1. Setup

A diagram of the experimental layout can be seen in Figure 3.1. The laser used was a Spectra Physics model 2040 argon ion laser. The laser's output was adjusted to single mode operation at 514.5 nm by utilizing an intercavity etalon. The 514.5 nm line was selected because it was experimentally proven to have the highest reflectivity. [Ref. 12]

As depicted in Figure 3.1, the laser's output was reflected off of two mirrors (M1 and M2) because of the physical arrangement of the laboratory. A 50% beam splitter (B.S.) was used to divert half of the laser output to the $BaTiO_3$ crystal. The other half of the laser output was directed to a 0.85 m SPEX Double Spectrometer. The spectrometer measured laser intensity as a function of wavelength.

A Stanford Research Systems SR540 optical chopper was inserted after the mirrors to square-wave modulate the intensity of the argon-ion laser. The chopper rotated at a frequency of 400 Hz (2400 RPM) and had six apertures of 0.84 inches evenly spaced around the circumference of the blade. The reference signal of chopper frequency was provided to a SR510 Lock-in Amplifier. The lock-in amplifier provided phase synchronization between the laser input signal and the output of the double spectrometer so that maximum amplitude was measured and random noise was filtered out. The measured signals was recorded on a model 7090A Hewlett Packard measurement plotter.
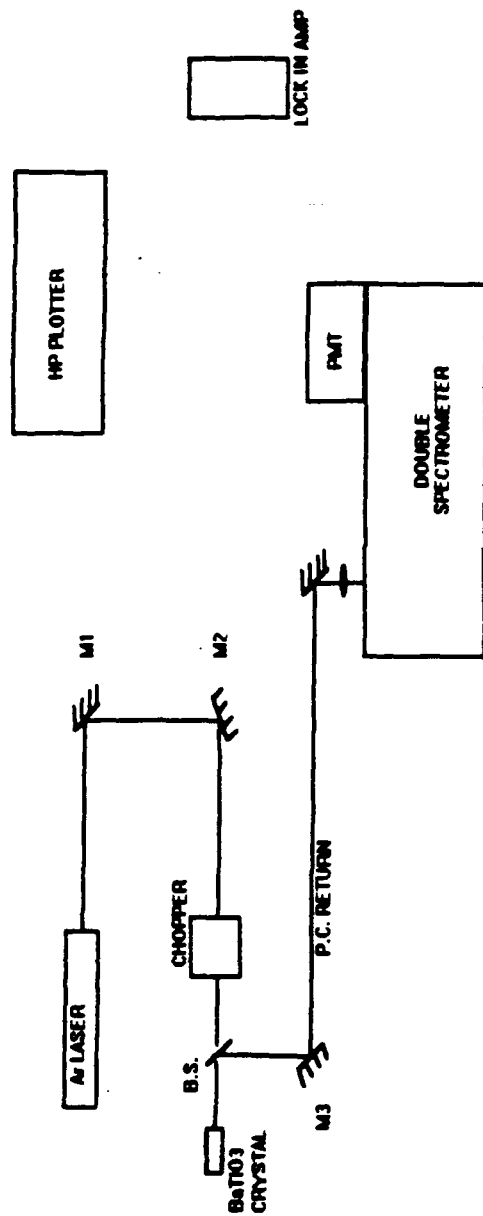
27

Figure 3.1. Self-pumped phase conjugation experimental diagram.

28

2. Procedure

After the laser was energized the spectrum was measured only on the laser output. The output is shown in Figure 3.2. The curve in the figure is not characteristic of a normal Gaussian or Lorentzian shaped laser output but is characteristic of the double spectrometer's measuring capability. The individual laser line at 514.5 nm is buried in the high intensity portion of the curve. The double spectrometer used for these experiments was normally used to measure phosphorescence of organic dyes. The spectrometer unfortunately did not have the sensitivity and resolution capability that was needed to measure the linewidth of the 514.5 nm line.

After the laser's spectrum was measured, the experiment's configuration was changed to measure the spectrum of the phase conjugate signal. The path length of the phase conjugate signal to the spectrometer was compensated to that of the laser output to the spectrometer to minimize and path errors. The laser was energized and the crystal was illuminated. A phase conjugate return signal then appeared approximately 40 seconds after the laser illumination. The characteristic fanning beams were also observed inside the crystal. The phase conjugate return was then directed into the spectrometer and measured. The output is displayed in Figures 3.3 and 3.4. The curve in Figures 3.3 and 3.4 spread out more along the wavelength scale because of possible alignment changes of the returning beam relative to the slit of the double
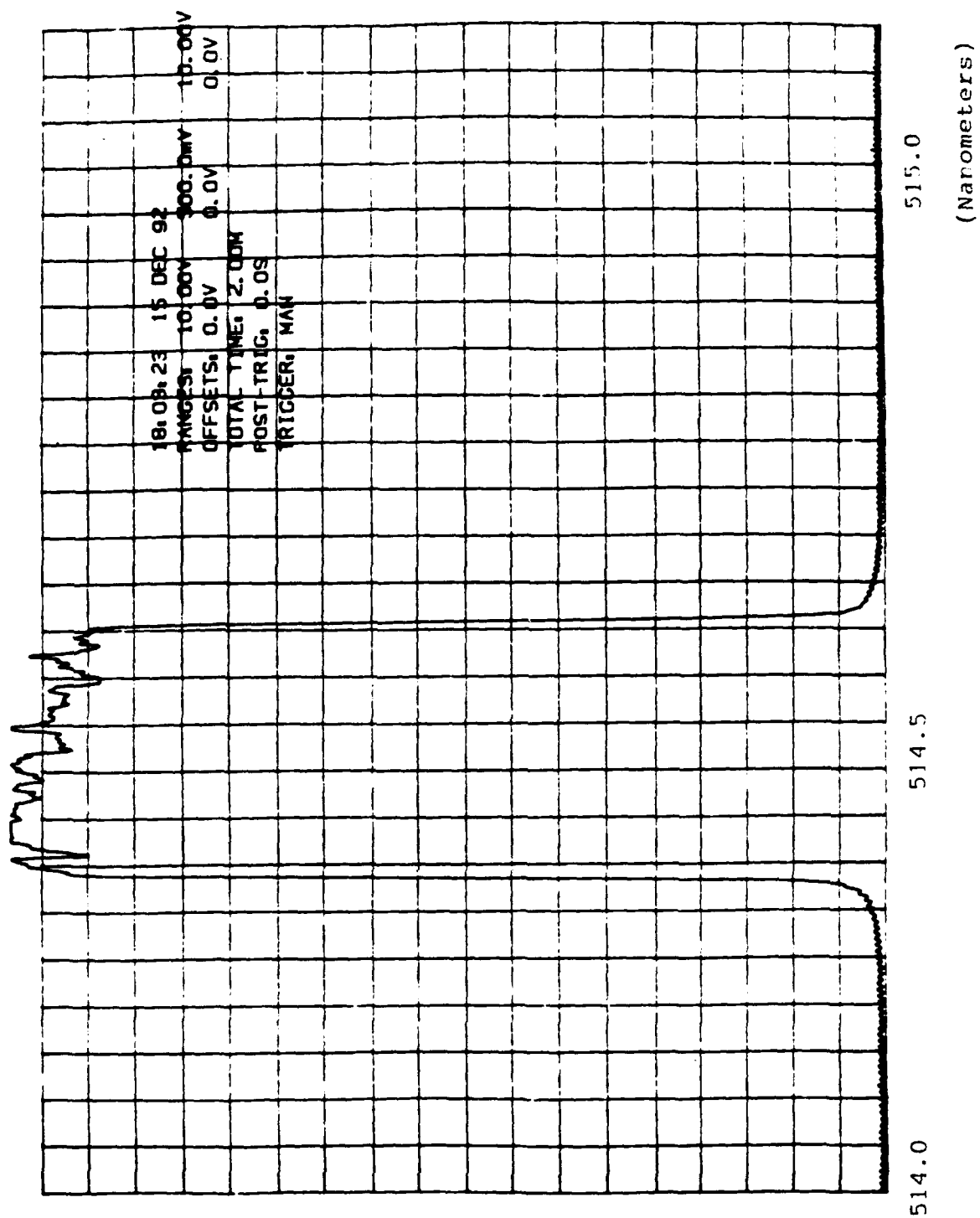
29

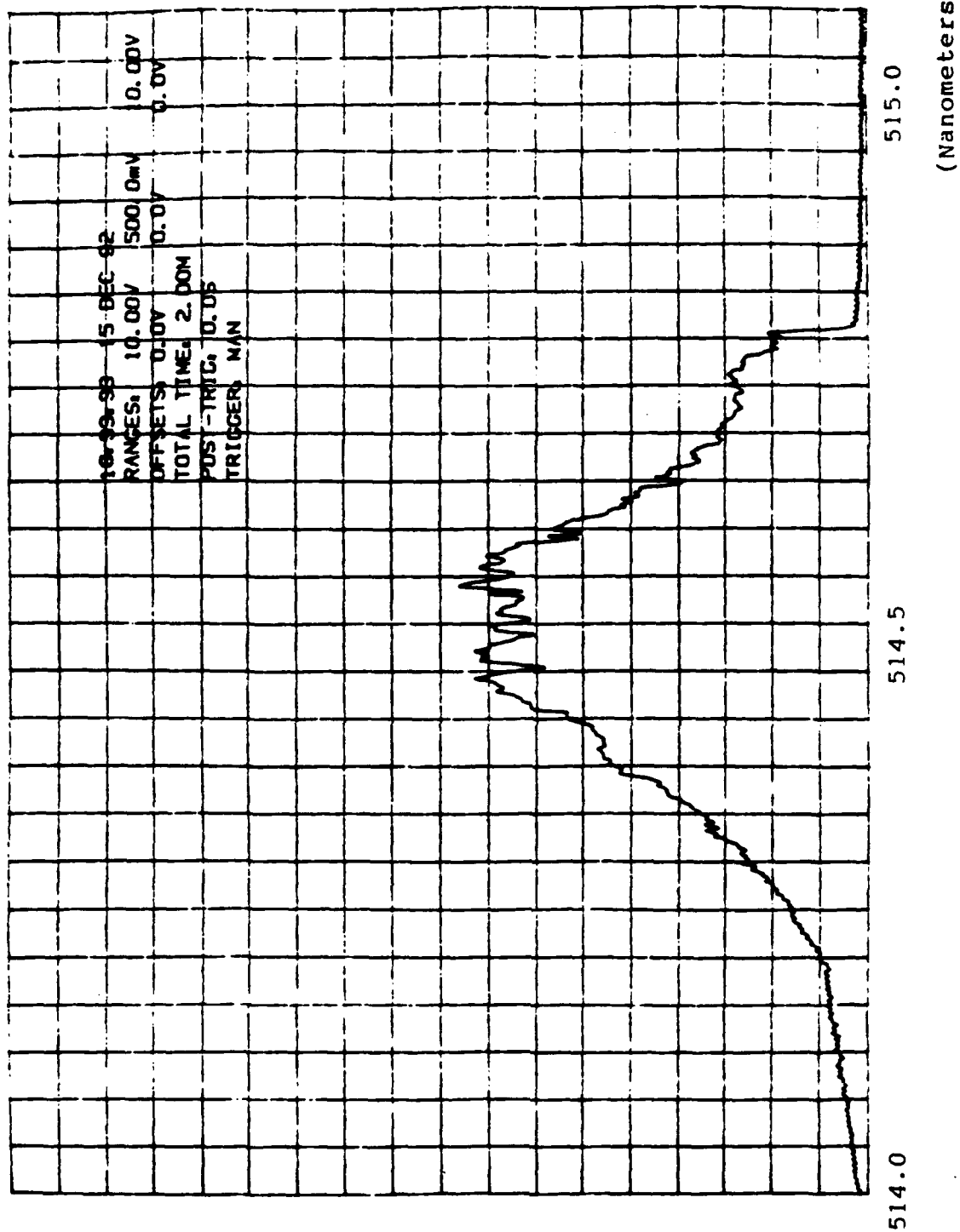**Figure 3.2.** Plot of relative intensity vs. wavelength of argon-ion laser.

30

Figure 3.3. Plot of relative intensity vs. wavelength of phase conjugate beam.
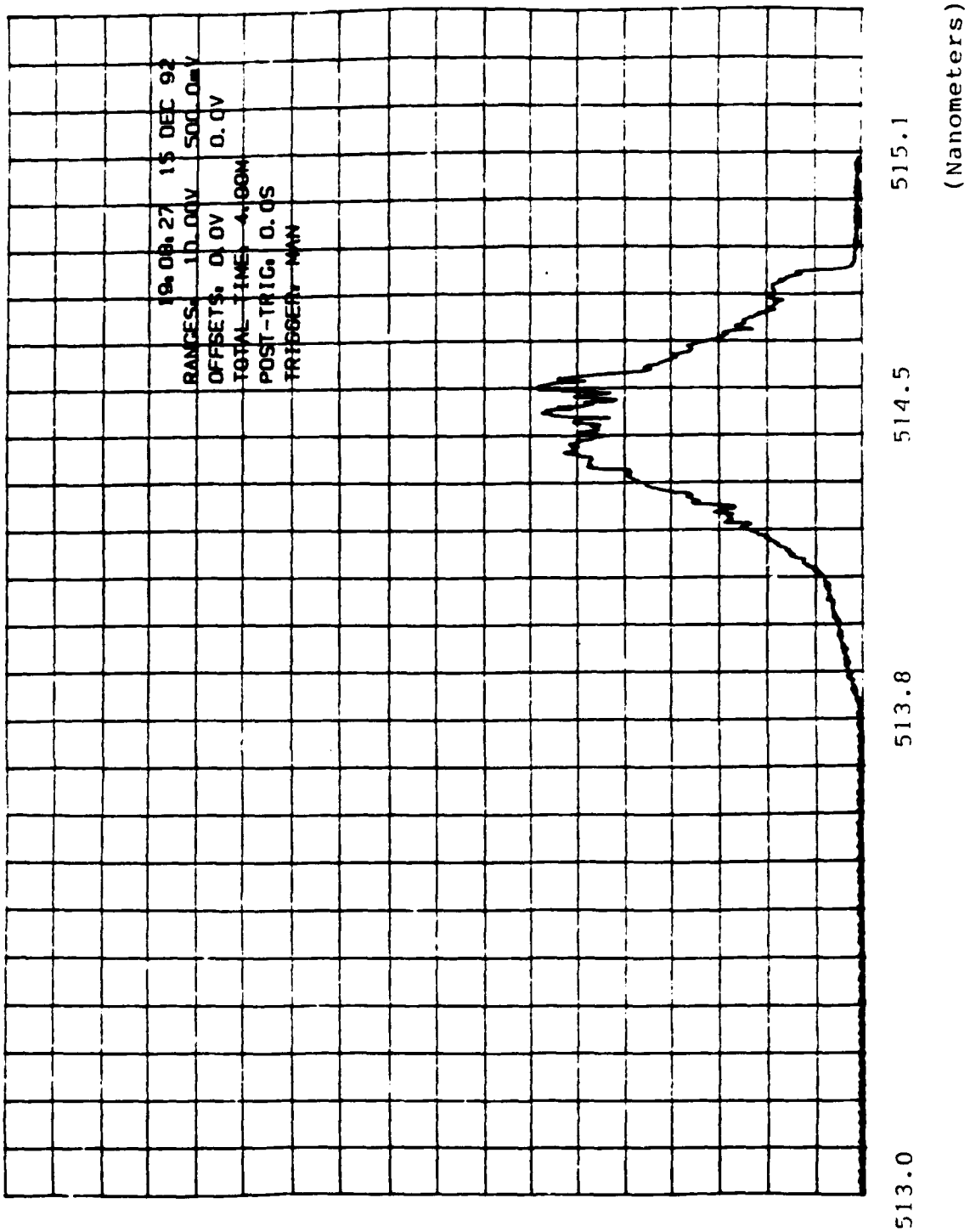
31

Figure 3.4. Plot of relative intensity vs. wavelength (extended scale) of phase conjugate beam.

spectrometer. Figure 3.4 shows the full effect of this spreading by pointing out the wavelength at which the spreading starts. The intensity axis for both measurements were normalized for comparison purposes. The intensity of the phase conjugate beam decreased approximately 75% from its original value. This reduction was possibly caused by excessive scattering within the crystal and a difference in alignments relative to the slit of the two beams. Again, the double spectrometer used to measure the temporal characteristics of the phase conjugate beam was not appropriate to measure laser linewidth.

C. CORNER CUBE REFLECTOR MEASUREMENTS

To compare the phase conjugate mirror's output to a conventional mirror, a second experiment was designed at the Naval Postgraduate School. This experimental arrangement involved a smaller argon-ion laser and a laser spectrometer that also measured a laser's spectrum . A corner cube reflector was used as the conventional mirror because it reflects light back along its incident path like a phase conjugate mirror.

1. Setup

The laser spectrometer utilized in this experiment was the Cynosure's LS-2 Laser Spectrometer. This spectrometer not only measures spectral width, but also possesses the capability of measuring wavelength, relative intensity, and separation between modes. A laser's wavelength can be determined to an accuracy of 0.01 nm. The laser source used was a Spectra Physics Model 162

argon-ion laser tuned to 514.5 nm at a power level of 5 mW. A schematic drawing of the experimental layout is shown in Figure 3.5.

2. Procedure

The first measurements were only made of the argon-ion laser. The laser output was directed into the aperture of the spectrometer and measured. The measured output was digitally interfaced to a Zenith Data Systems portable computer and recorded on an Epson FX-85 Printer. The measured data are displayed in Figure 3.6. After this baseline measurement was completed, the configuration in Figure 3.5 was used the measure the spectrum of the corner-cube reflector. The same recording procedure used previously on the baseline measurement was also utilized for the corner cube reflector. The spectrum measurement of the corner-cube reflector is displayed in Figure 3.7. The wavelength width of distribution ($\Delta\lambda$) at FWHM of the laser beam reflected from the corner cube reflector and the argon-ion laser can't be precisely measured because the wavelength scale does not provide enough resolution. This limitation was the result of an inadequate software package written for the spectrometer. After comparing these measurements with a standard ruler no appreciable differences in the spectral width could be discerned between the laser directly in and the laser reflected from the corner cube reflector.
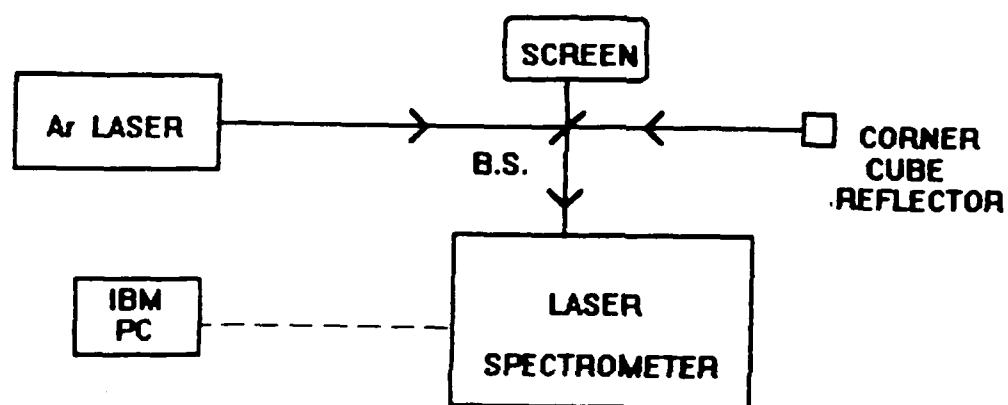
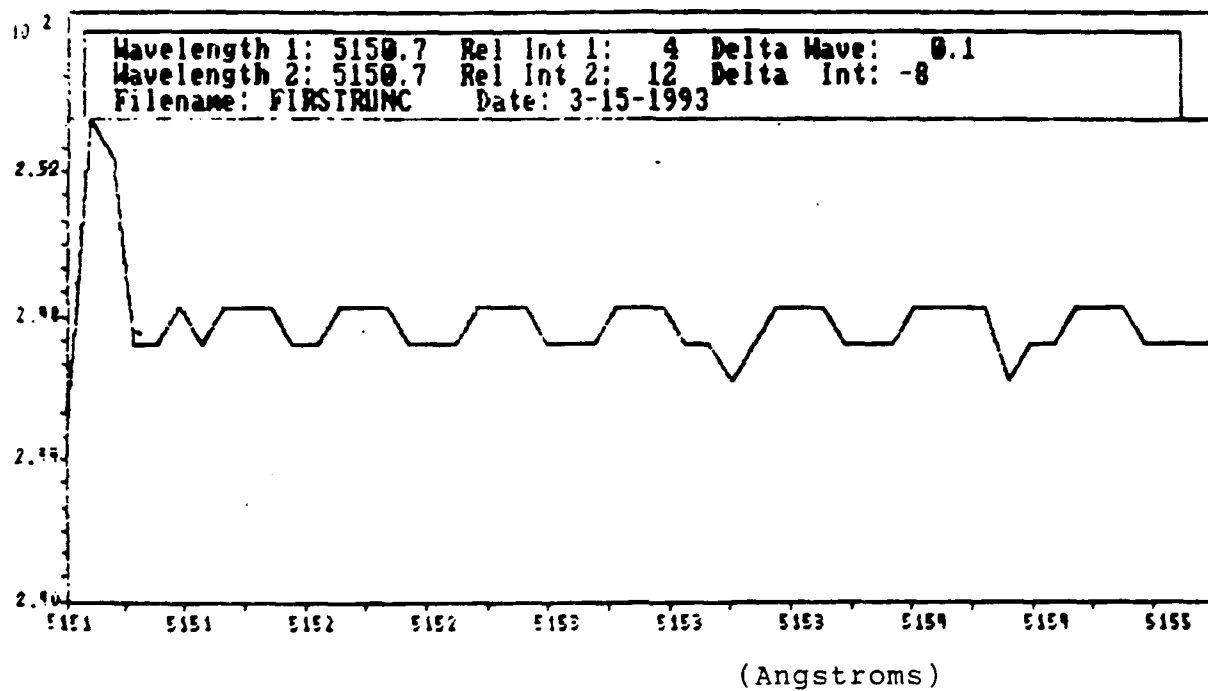**Figure 3.5.** Corner cube reflector experimental diagram.

Figure 3.6. Plot of relative intensity vs. wavelength of the argon-ion laser.
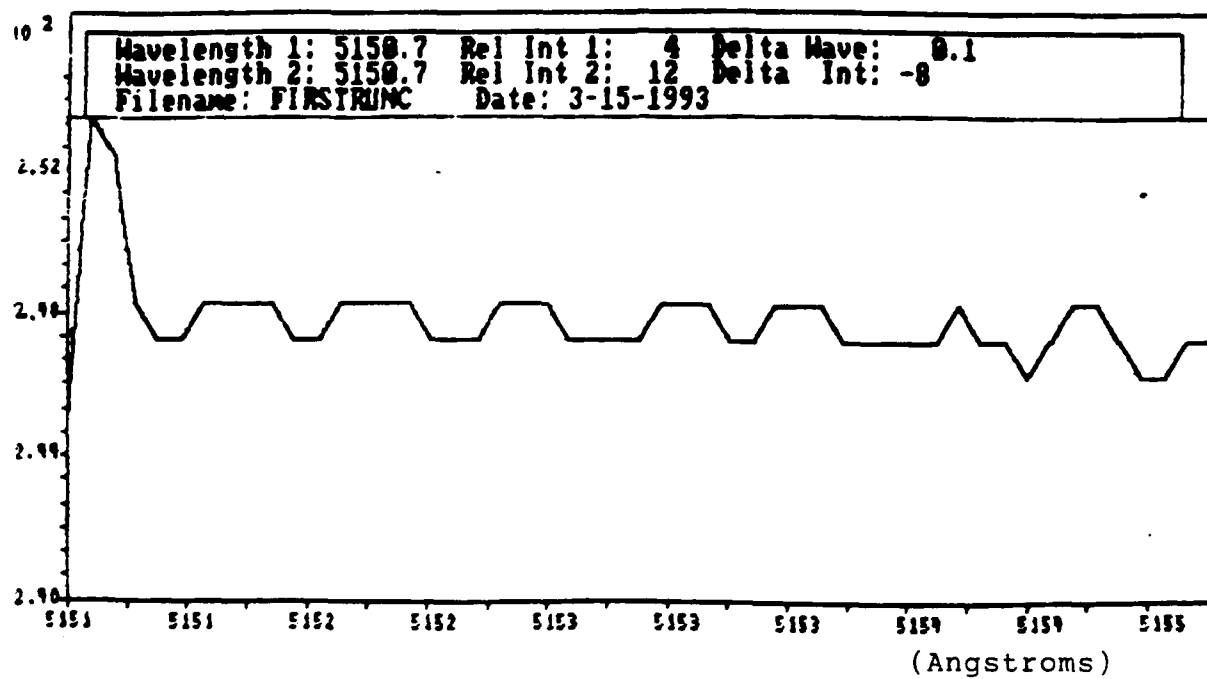
Figure 3.7. Plot of relative intensity vs. wavelength of the corner-cube reflector.

37

IV. DISCUSSION OF RESULTS

The results obtained in these experiments cannot confirm previous results obtained in experiments that involved changes in coherence length after phase conjugation. A self-pump phase conjugation experiment performed by Whitten and Ramsey [Refs. 13, 14] in which a dye laser was conjugated by $BaTiO_3$ revealed a decrease in spectral width. The spectral width was observed to decrease from 2.4 nm to 0.1 nm after a phase conjugate signal was established in the crystal. [Refs. 13, 14] This is the only documented (to our knowledge) experiment in which a change in coherence length was observed in a phase conjugate laser beam.

Experimental results obtained in these experiments highlight the fact that more precise spectrometers, such as a Fabry-Perot spectrometer, should be utilized to resolve a laser's linewidth. The first spectrometer, SPEX Double Spectrometer, was severely inadequate in measuring laser linewidth. Another disadvantage of the SPEX was that the two separate laser beams had to be perfectly aligned at the same location relative to the spectrometer's slit so that consistent measurements were taken. The second spectrometer, Cynosure's LS-2, was more capable than the SPEX model but was limited by the software interface. The manufacturer is in the process of upgrading the software package for the spectrometer. The new package will include a more capable resolution calculation

and display of wavelength and laser linewidth. As with the SPEX, the LS-2 spectrometer possessed some alignment limitations. These limitations weren't as severe as with the SPEX because both the slit and grating were much smaller.

Interference effects due to feedback from the BaTiO$_3$ crystal were neglected in these experiments. However, for future experiments, these effects should be eliminated to permit the examination of a pure phase conjugate beam. By placing a Faraday isolator between the laser and the crystal, the feedback caused by the phase conjugate return interfering with the laser cavity modes will be prevented.

V. CONCLUSIONS AND RECOMMENDATIONS

The experimental results obtained in this study were inconclusive in determining that a "penalty" exist in the self-pumped phase conjugation process. To measure the coherence length of a self-pumped phase conjugated beam, a Fabry-Perot spectrometer or a Michelson interferometer should be utilized. Measurements made by conventional spectrometers did not possess the required resolution to effectively measure laser linewidth.

Results obtained from the corner-cube reflector measurements indicate that, while this is not a true phase conjugation, losses are very small or nonexistent in ordinary specular reflections. As a result, there were no appreciable changes in coherence length or intensity that could be determined with quantitative measurements. Additional experiments should be performed to verify the above premise with ˙∟gher resolution spectrometers.

Future experiments in this area should include the examination of laser coherence length changes after conjugation with a Fabry-Perot spectrometer or Michelson interferometer. A Faraday isolator should be placed between the laser and the crystal prior to taking any measurements of the phase conjugate return. Also, coherence length differences after conjugation should be analyzed in other conjugating media such as organic materials and high pressure gases.

Additionally, the conjugate beam obtained in photorefractive four wave mixing should be examined specifically for any change in coherence length.

LIST OF REFERENCES

1. Biblarz, O., *Untitled Paper*, Naval Postgraduate School, 1992.

2. Fisher, R.A., *Optical Phase Conjugation*, Academic Press, Inc., 1983.

3. Pepper, D.M., *Nonlinear Optical Phase Conjugation*, Elsevier Science Pubishers, 1985.

4. Shen, Y.R., *The Principles of Nonlinear Optics*, Wiley and Sons, 1984.

5. Rayn, J.R., *Optical Phase Conjugation via Four-Wave Mixing in Barium Titanate*, Master's Thesis, Naval Postgraduate School, March, 1986.

6. Gunter, P., *Electro-Optic and Photorefractive Materials II*, Spring-Verlag Publishers, 1987.

7. Yeh, P., "Photorefractive Phase Conjugators," *Proceedings of the IEEE*, v. 80, pp. 436-450, 1992.

8. Feinberg, J., "Self-Pumped Continuous Wave Phase Conjugator Using Internal Reflection," *Optics Letters*, v. 7, pp. 486-489, 1982.

9. Dokhanian, M., *Optical Phase Conjugation by Barium Titanate*, Ph.D. Dissertation, Alabama A&M University, Huntsville, Alabama, February, 1992.

10. Yariv, A., *Quantum Electronics*, 3rd Ed., Wiley and Sons, 1987.

11. Hecht, J., *Understanding Lasers—An Entry Level Guide*, IEEE Press, 1992.

12. Jahoda, F.C., Weber, P.G., and Feinberg, J., "Optical Feedback, Wavelength Response, and Interference Effects of Self-Pumped Phase Conjugation in BaTiO$_3$," *Optics Letters*, v. 9, pp. 362-364, 1984.

13. Ramsey, J.M., and Whitten, W.B., "Phase Conjugate Feedback Into a Continuous Wave Ring Dye Laser," *Optics Letters*, v. 7, pp. 362-364, 1985.

14. Whitten, W.B., and Ramsey, J.M., "Self-Scanning of a Dyle Laser Due To Feedback From a BaTiO$_3$ Phase Conjugate Reflector," *Optics Letters*, v. 9, pp. 44-46, 1984.

15. Siegman, A.E., *Lasers*, University Science Books, 1986.

16. Ewbank, M.D., and Yeh, P., "Frequency Shift and Cavity Length in Photorefractive Resonators," *Optics Letters*, v. 10, pp. 496-498.

APPENDIX. POSSIBLE MECHANISIMS OF BROADENING IN BaTiO₃

There are several mechanisms or interactions which could cause line broadening of a phase conjugated beam. The most probable cause of this spectral broadening is phonon broadening within the crystal. Phonon broadening is the rapid the random frequency modulation of an atom in a solid. The frequency modulation is caused by lattice vibrations in the surrounding crystal lattice. [Ref. 15] The vibration quantum energy levels coincide with the laser's energy levels thus causing the laser to transfer energy to the crystal. Phonon broadening does depend on lattice temperature because the lattice vibrations result from thermal excitation of the lattice modes. [Ref. 15] Lattice temperature effects were not studied in this experiment but would be an excellent topic for future study.

Another possible process that can add to line broadening is dipolar broadening. Dipolar broadening results from the random interaction and coupling between nearby atoms in a crystal because of overlapping dipolar electric and magnetic fields. These fields cause random oscillations of the crystal's atomic dipoles. If these oscillation energies coincide with the transition energies of the laser, line broadening can occur. Unlike phonon broadening, dipolar broadening does not depend on lattice temperature. [Ref. 15]

In previous experiments involving interferometry of self-pumped phase conjugators, a frequency shift of approximately 1 Hz was observed on the phase

conjugate return beam. [Ref. 16] This frequency shift was attributed to moving

photorefractive gratings formed inside the crystal of $BaTiO_3$. It can be postulated

that these gratings scatter laser photons thus reducing the amount of in-phase

returning radiation and subsequently broadening the spectral width.

INITIAL DISTRIBUTION LIST

		No. Copies
1.	Defense Technical Information Center Cameron Station Alexandria, Virginia 22304-6145	2
2.	Library, Code 52 Naval Postgraduate School Monterey, California 93943-5002	2
3.	Prof. O. Biblarz, Code AA/Bi Naval Postgraduate School Monterey, California 93943-5000	2
4.	Prof. D. L. Walters, Code PH/We Naval Postgraduate School Monterey, California 93943-5000	1
5.	Prof. A. W. Cooper, Code PH/Cr Naval Postgraduate School Monterey, California 93943-5000	1
6.	Prof. B. Agrawal, Code AA/Ag Naval Postgraduate School Monterey, California 93943-5000	1
7.	Chairman Space Systems Academic Group, Code SP Naval Postgraduate School Monterey, California 93943-5000	1
8.	Chairman Department of Physics, Code PH Naval Postgraduate School Monterey, California 93943-5000	1

9.   Dr. Hossin Abeledeyem   1
      Space Science Laboratory, Code ES74
      Marshall Space Flight Center
      Huntsville, AL 35812

10.   LT George M. Sutton   2
      721 Pennsylvania ST
      New Roads, LA 70760